

## ON THE ORIGIN OF LONG SECONDARY PERIODS IN SEMIREGULAR VARIABLES

E. A. OLIVIER AND P. R. WOOD

Research School of Astronomy and Astrophysics, Australian National University, Cotter Road, Weston Creek, ACT 2611, Australia

Received 2002 May 2; accepted 2002 October 22

### ABSTRACT

The presence of a long secondary period (LSP) in the light curves of some local semiregular variables has been known for many years. Furthermore, the LSPs have recently been found in the light curves of approximately 25% of the semiregular variables in the LMC. They typically have a length of  $\sim 500$ – $4000$  days, some 5–15 times longer than the primary period. Binarity, pulsation, periodic dust ejection, and rotation have been suggested as the origin of the LSPs. Here we analyze echelle spectra of a group of local semiregular variables with LSPs (hereafter LSPVs) in order to try to distinguish between these suggestions. In general, we find that LSPVs do not have broader spectral features than semiregulars without a long secondary period (hereafter non-LSPVs). The general upper limit on the equatorial rotation velocity of  $3 \text{ km s}^{-1}$  rules out rotating spot and similar models. One LSPV, V Hya, does have broader spectral lines than similar carbon stars, but it is shown here that rotation alone is not a good model for explaining the broad lines. Mid-infrared colors of LSPs and non-LSPVs are similar and there are no LSPVs showing the large (60–25)  $\mu\text{m}$  *IRAS* color exhibited by some R Coronae Borealis (RCB) stars. Thus, there is no evidence for periodic dust ejection from LSPVs. Finally, we find that the LSPVs show larger radial velocity variations than non-LSPVs, which suggests that LSPs are caused either by binarity or by pulsation. A similar conclusion was derived by Hinkle and co-workers.

*Subject headings:* infrared: stars — Magellanic Clouds — stars: variables: other

### 1. INTRODUCTION

It has been known for a long time that some local semiregular variables show the presence of a long secondary period (LSP) in their light curves, typically 5–15 times longer than the primary pulsation period (Houk 1963). Houk (1963) lists 103 such local semiregular variables while Kiss et al. (1999) list some further objects and show examples of light curves. Recently, Wood et al. (1999, hereafter W99), studied a group of red variables in the LMC using MACHO data and discovered that about  $\sim 25\%$  of them show a long secondary periodic variation.

Possible explanations for the LSPs include pulsation, rotation combined with surface irregularities, binary companions, and episodic dust ejection (see W99 and Wood 2000a). There is some evidence in favor of each of these suggestions. (1) W99 noted that the period-luminosity relation they saw could be explained by the asymptotic giant branch (AGB) star being in a semidetached binary system. In this scenario the AGB variable fills its Roche lobe, losing mass to its companion. This forms a dusty cloud of matter around the companion, which then obscures the star each time it crosses the line of sight. (2) Barnbaum, Morris, & Kahane (1995) found evidence for spectral broadening in V Hya, a known local semiregular variable with an LSP (hereafter LSPVs), and attributed this to rapid rotation. The rotation velocity ( $\sim 6$ – $16 \text{ km s}^{-1}$ ) seem to vary with the same period as the pulsation. They suggested that the LSP of V Hya of about 6200 days could be attributed to a coupling of the radial pulsation (530 day period) with rotation. (3) Olivier, Whitelock, & Marang (2001) showed V Hya to be reddened during the LSP variations. The LSP amplitudes are 2.4, 2.1, 1.7, and 0.7 mag at *J*, *H*, *K*, and *L*, respectively, while the *V* amplitude is  $\sim 3.5$  mag (Knapp et al. 1999). It is not clear why the interaction suggested by Barnbaum et al. (1995) would give rise to the observed reddening, while the reddening could easily follow from the scenario presented by W99 or from episodic dust ejection in events of the type

found by Winters et al. (1994) and Höfner, Feuchtinger, & Dorfi (1995). (4) The presence of large star spots on the surface of AGB stars has been suggested by Schwarzschild (1975), the cool regions being associated with very large convective elements. Recently, the presence of cool magnetic spots on AGB stars has been proposed (see, e.g., Soker & Clayton 1999). Combined with rotation, such spots could explain the LSPs: a typical AGB star with a radius of  $300 R_{\odot}$  and a rotation velocity of  $10 \text{ km s}^{-1}$  (about one third the break-up velocity), with a large star spot, will give rise to a secondary period of  $\sim 1500$  days.

We note that the rotation velocities of  $\sim 10 \text{ km s}^{-1}$  mentioned above cannot easily be explained as rotation inherited from the main-sequence phase. A  $1 M_{\odot}$  progenitor rotating at break-up velocity on the main-sequence will give rise to a  $300 R_{\odot}$  AGB star rotating at only  $\sim 1 \text{ km s}^{-1}$ . It is therefore necessary to invoke binary mass and angular momentum transfer, probably a binary merger, in order to get rotation velocities larger than  $\sim 1 \text{ km s}^{-1}$ . For example, a binary system with each member having a mass of  $1.2 M_{\odot}$  and a separation of  $150 R_{\odot}$  that merges to a single star of radius  $300 R_{\odot}$  (conserving mass and angular momentum) will rotate with a period of  $\sim 900$  days and equatorial surface rotation velocity of  $\sim 17 \text{ km s}^{-1}$ .

In this paper, we examine high-resolution spectra of a sample of LSPVs and a similar sample of non-LSPVs in order to look for evidence of rotation and/or radial velocity variations due to binary motion or pulsation. The spectra are part of an on-going monitoring program for these stars. We also examine *IRAS* data for the sample in order to look for evidence of the dust that might be expected around LSPVs in some of the scenarios listed above.

### 2. SAMPLE AND OBSERVATIONS

A sample of 26 local LSPVs, nine C-type and 15 M-type, were selected from the list of Houk (1963) for observation. These are listed in Table 1 together with spectral and

TABLE 1  
THE SAMPLE OF LSPVs

Name	Spectral Type	Variable Type	$P_{\text{puls}}$ (day)	LSP (day)	Name	Spectral Type	Variable Type	$P_{\text{puls}}$ (day)	LSP (day)
Z Eri .....	M5 III	SRb	80	746	V574 Oph.....	M4	SRa	72	500
V Eri .....	M5/M6 IV	SRb	97	1209	RT Pav.....	M4/M5 III	SR	85	757
S Lep.....	M5 III	SRb	90	883	EI Del .....	M2	SRb	20	600
SX Mon.....	M6.5	SR	100	1100	BM Aqr .....	M3 III	SRb	60	550
CO CMa.....	M3 IIIe	SRb	80	700	W Ori.....	C II	SRb	212	2450
RT Cnc.....	M5 III	SRb	90	542	RT Ori.....	C II	SRb	321	3200
SY Vel.....	M5/M6 III	SRb	63	1400	RV Mon.....	C II	SRb	132	1047
SU Hya.....	M4 III	SRb	95	780	Y Hya .....	C	SRb	95	1200
BZ Car.....	M3	SRb	97	1800	V Hya .....	C	SRa	533	6160 ± 400
T Crt.....	M6 III	SRb	70	1006	T Mus.....	C	SR	93	1021
AN Vir.....	M6 III	SRb	100	1000	TW Oph.....	C II	SRb	165	2000
W Nor.....	M4/M5 III	SRa	135	1300	V Pav.....	C	SRa	225	3735
V521 Oph.....	M	SRb	320	3500	V Aql.....	C II	SRb	353	2270

NOTES.—Periods are taken from Houk 1963, except for V Hya whose LSP is taken from Knapp et al. 1999. Spectral types are from *SIMBAD* and variable types are from the GCVS.

variable type, primary pulsation period, and LSP. Table 2 lists the same data for a similar control group of 30 semi-regulars, 20 M-types and 10 C-types, showing no LSP, that were selected from the General Catalogue of Variable Stars (Kholopov 1985, hereafter GCVS) as being in the same part of the sky as the LSPVs. As can be seen from Tables 1 and 2, pulsation periods range from ~50–300 days and LSPs from ~500–4000 days (excluding V Hya). The Kolmogorov-Smirnov (KS) two-sample test gives a probability of 70% that both samples came from the same parent population in pulsation period, i.e., no significant differences in pulsation period exists between the two groups.

Here we examine echelle spectra obtained for the objects listed in Tables 1 and 2 during nine nights over a period of about 1 yr. The spectra were taken with the Coude Echelle spectrograph (31 line mm<sup>-1</sup> echelle grating) on the 74" telescope at Mount Stromlo Observatory. The detector was an SITE 2048 × 4096 CCD with 15 μm pixels. The dispersion of the spectra is 1.52 km s<sup>-1</sup> pixel<sup>-1</sup>, with a central wavelength

of 6563 Å (Hα). The resolution is typically 2.75 pixels. Not all objects were observed with the same frequency, in particular only 17 of the non-LSPVs were observed on more than one night. In total 132 high-resolution echelle spectra were obtained.

The data were reduced with the IRAF software package. The raw images were bias subtracted and any bad pixels on the CCD were fixed, using standard CCD reduction procedures in IRAF. The images were then flat-fielded and the wavelength-calibrated spectra were extracted using the IRAF task *doecslit*. Figure 1 shows examples of typical M-type and C-type stellar spectra obtained.

### 3. SPECTRAL LINE BROADENING AND ROTATION

As mentioned earlier, Barnbaum et al (1995) found evidence for spectral broadening in the LSPV V Hya by comparing its spectrum to that of several other similar carbon stars, in particular U Hya, and suggested the

TABLE 2  
THE SAMPLE OF SEMIREGULARS WITHOUT AN LSP

Name	Spectral Type	Variable Type	$P_{\text{puls}}$ (day)	Name	Spectral Type	Variable Type	$P_{\text{puls}}$ (day)
AG Cet .....	M5 III	SRb	90	V763 Cen .....	M3 III		60
SU Eri.....	M4 III	SRb	112	V Aqr.....	M6e	SRa	244
RR Eri.....	M5 III	SRb	97	SZ Vel.....	M5	SRb	150
T Cae.....	C II	SR	156	CK Car.....	M3.5	SRc	525
RX Lep.....	M6 III	SRb	60	U Hya.....	C II	SRb	450
Y Tau.....	C II	SRb	242	RR Crt.....	M5	SRb	
GK Ori.....	N	SR	236	RR Mus.....	C	SRb	75
RY Mon.....	N	SRa	456	EV Vir.....	M3 III	SRb	120
GH CMa.....	M4 III	SRb	20	V Nor.....	M6 III	SRb	156
BP Cnc.....	M3 III	SRb	40	V515 Oph.....	M	SRb	304
GO Vel.....	M4 III	SRb	75	V520 Oph.....	M	SRd	117
AK Hya.....	M6 III	SRb	75	TY Oph.....	N	LB	
IN Hya.....	M3	SRb	65	Y Pav.....	C II	SRb	233
IO Hya.....	M4 III	SRb	80	SX Pav.....	M5 III	SRb	50
RW Cen.....	C	SRa		UV Aql.....	C II	SRa	385

NOTES.—Periods and variable types are taken from the GCVS. Spectral type are from *SIMBAD*, except for V515 Oph and V520 Oph for which spectral types were inferred from the spectra taken in this study.

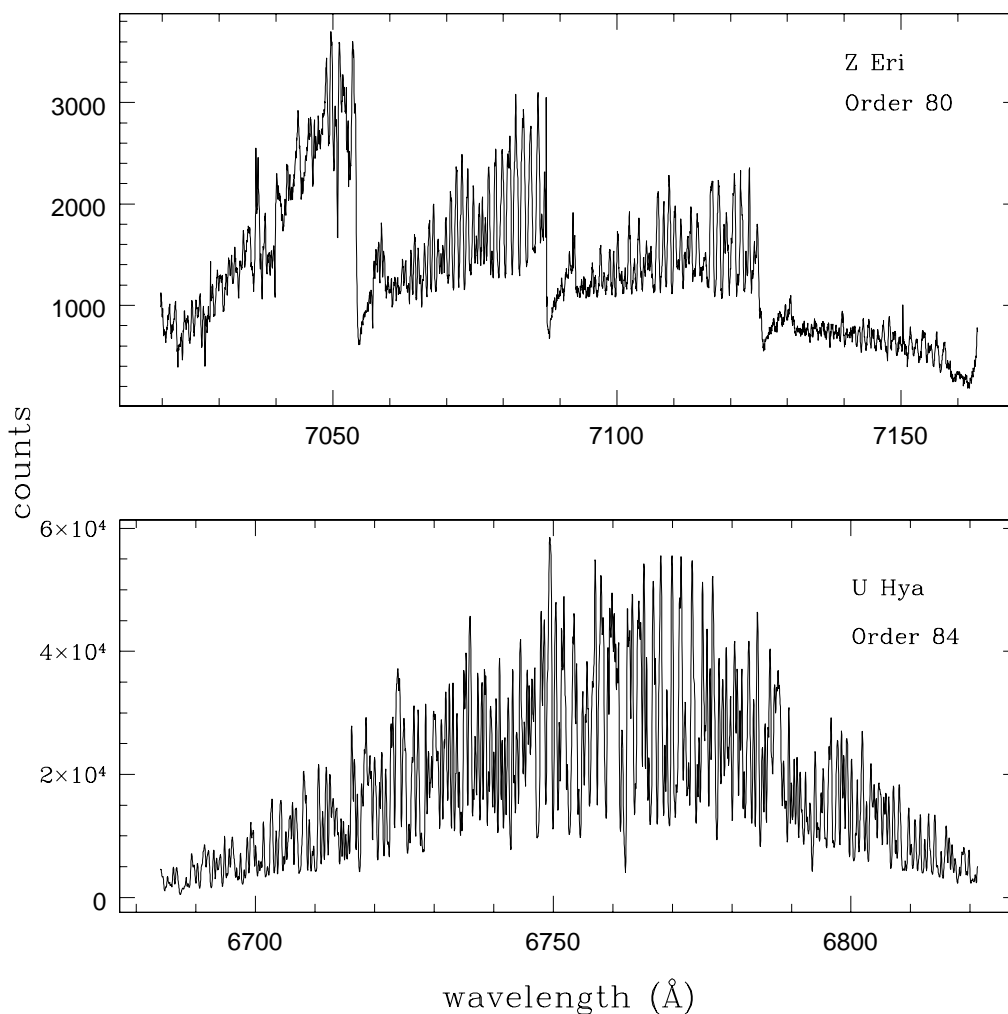


FIG. 1.—Spectra for two variables Z Eri (M-type) and U Hya (C-type). The spectrum of Z Eri clearly shows the TiO band heads, which are characteristic of M star spectra. Note that these spectra are not corrected for heliocentric motion.

difference might be due to rotation. Figure 2 shows the Fourier power spectra of V Hya and U Hya. The power spectrum of U Hya broadened with a line-of-sight rotation velocity of  $8 \text{ km s}^{-1}$  and a limb-darkening coefficient of 0.8 is also shown in Figure 2 (the broadening was done according to the rotational broadening model described in Gray 1976). This power spectrum seems to fit the power spectrum of V Hya fairly well over lower frequencies ( $\sim 0\text{--}2 \text{ cycles } \text{\AA}^{-1}$ ), but at higher frequencies ( $\sim 2.5\text{--}4 \text{ cycles } \text{\AA}^{-1}$ ) the fit is not good; i.e., rotation alone is not a good model for the broadening seen in V Hya. A macroturbulence model, with the turbulent elements having different radial and tangential velocity distributions, may lead to a better fit. Such a model will have more power at higher frequencies than a simple rotation model (see, e.g., Fig. 18-9 in Gray 1976).

All stars in our sample have been examined for the presence of broadening caused by rotation. The M-type stars were divided into three groups, according to a spectral type index,  $R$ , which is simply the ratio of the flux in a  $10 \text{ \AA}$  waveband shortward and longward of the TiO band head at  $7050 \text{ \AA}$ . Power spectra calculated from the flux spectra (all stars at different dates), with a noise-to-power ratio at 2 cycles

$\text{\AA}^{-1}$  of less than  $\sim 5\%$  are shown in Figure 3. The spectra are grouped by spectral type.

The main effect of rotation on the power spectrum is to alter the overall slope (as seen in Fig. 2). In order to estimate the slope, a simple curve of the form  $\log p = \text{const.} - \alpha \sigma^2$  (where  $p$  is the power and  $\sigma$  is in units of  $\text{cycles } \text{\AA}^{-1}$ ) was fitted to each power spectrum in Figure 3, with  $\alpha$  thus being an indicator of the slope. The fitting was done by least-squares minimization over the range  $0.4\text{--}3.5 \text{ cycles } \text{\AA}^{-1}$ . Figure 4 shows the mean values of  $\alpha$  for each group. Also shown is the Student  $t$ -test statistic  $t$  and the associated probability,  $p_t$ , that the values of  $\alpha$  for non-LSPVs and LSPVs are drawn from distributions with the same mean. It is clear that there is no significant difference in  $\bar{\alpha}$  for LSPVs and non-LSPVs for groups 3 and 4. The differences for groups 1 and 2 are significant at the 5% level, with the non-LSPV power spectra having a *steeper* slope than those of the LSPVs, in the mean. Within the context of the rotation model, this suggests *less* rotation in LSPVs than non-LSPVs, certainly not in agreement with the suggestion that the LSPs may originate from rotation. In general, looking at Figure 4, it seems that the LSPVs in groups 1 and 2 have

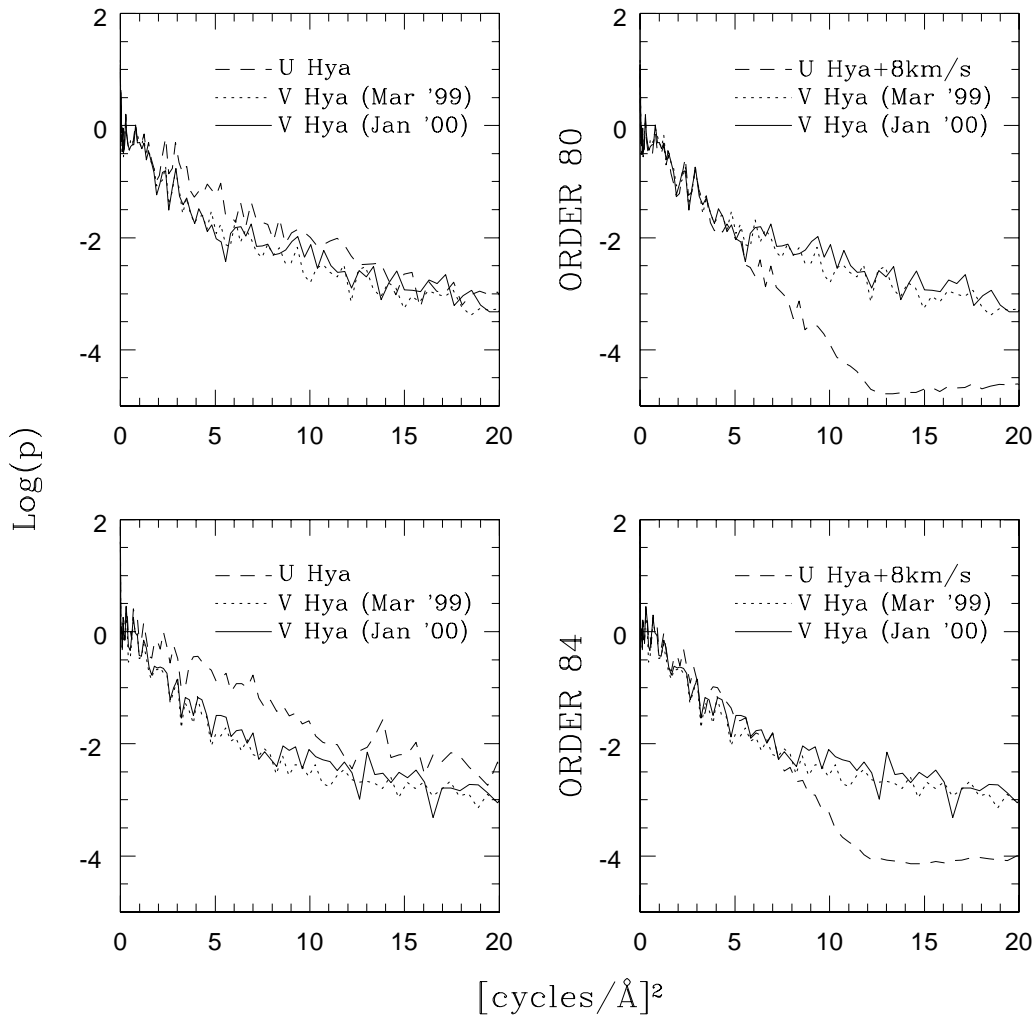


FIG. 2.—Power spectra of the flux spectra of U Hya and V Hya plotted against the square of the frequency. The top and bottom panels are for orders 80 (7030–7160 Å) and 84 (6700–6800 Å), respectively. *Left panels*: unbroadened spectra of U Hya. *Right panels*: rotationally broadened spectra of U Hya with the noise of the original power spectrum added. Power spectra are normalized at  $0.5 \text{ cycles } \text{Å}^{-1}$ .

more power at higher frequencies ( $3\text{--}4 \text{ cycles } \text{Å}^{-1}$ ) than the corresponding non-LSPVs. This suggests that the LSP phenomenon in some way decreases line broadening. Possibilities include a reduction in the pulsation velocity or velocity gradient in the stellar atmosphere or more prominent lines from the cooler parts of the photosphere where there is less thermal broadening.

To quantify the limits the present results put on the rotation in LSPVs, we note by examining Figure 4 that a  $2\sigma$  uncertainty in  $\bar{\alpha}$  corresponds to 0.02. The rotation model of Gray shows that a  $3.0 \text{ km s}^{-1}$  equatorial rotation velocity would increase  $\bar{\alpha}$  by 0.02 (a  $5 \text{ km s}^{-1}$  velocity would increase  $\bar{\alpha}$  by 0.06). Given the actual observed *decrease* in  $\bar{\alpha}$ , we can very conservatively rule out rotation velocities greater than  $3 \text{ km s}^{-1}$  as a general characteristic of LSPVs.

Given that these stars have radii of  $\sim 170 R_{\odot}$ , a  $3 \text{ km s}^{-1}$  rotation velocity would give a rotation period of 2868 days. Since only four of the 28 LSPVs here have secondary periods longer than 2868 days, the rotation period cannot generally be equated to the LSP. This rules out rotating spot models for the LSPVs. Even rotating stars of dipolar shape (whose observed period would be half the rotation period) are ruled out in most cases as well.

#### 4. RADIAL VELOCITY VARIATIONS

The large number of molecular absorption lines present in the spectra of these late-type stars make it possible to determine very accurate relative radial velocities via cross-correlation. Heliocentric velocities were calculated for each star on multiple dates. Then the velocity changes  $v_r'$  relative to a specific date were computed for each star. The velocity changes were calculated using order 80 ( $\sim 7020\text{--}7160 \text{ Å}$ ). Other orders (wavelength ranges) were used as well to cross check, and these velocities agreed to better than  $0.3 \text{ km s}^{-1}$ . The velocity changes that occurred for each star are shown as a histogram in Figure 5, with separate histograms for the LSPV and non-LSPV groups.

It is clear that the distribution of LSPV velocity changes is broader than that of the non-LSPVs. The KS two-sample test gives a probability that the two distributions came from the same parent population of less than 0.02, i.e., the two distributions are significantly different. Note that the width of the non-LSPV histogram is a measure of the pulsation velocity associated with the pulsation in these SR variables: the LSPV histogram width will have a pulsation component similar to that of the non-LSPV histogram. The larger

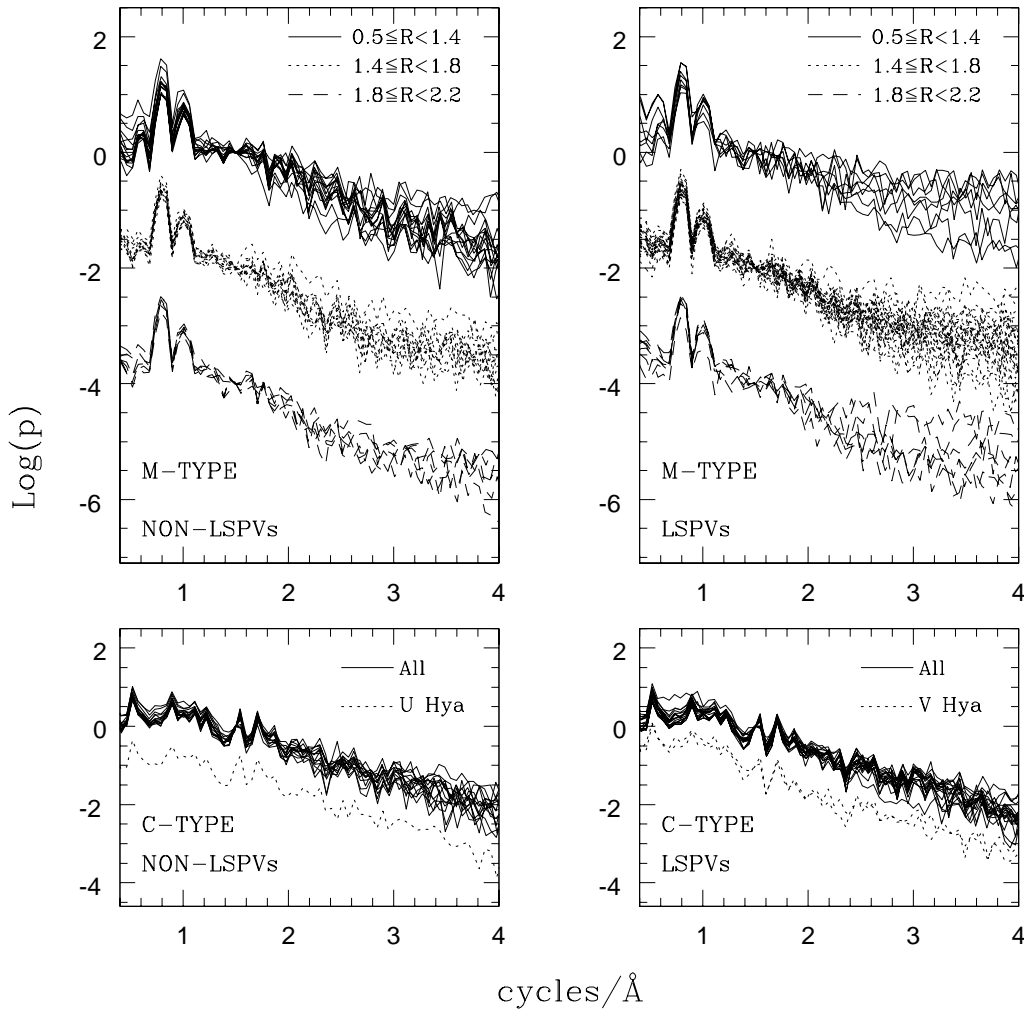


FIG. 3.—Power spectra calculated in the wavelength range of 7030–7160 Å (order 80). Power spectra are normalized at 1.5 cycles Å<sup>-1</sup>. The index  $R$  is described in the text.

velocity changes in the LSPVs could be due to binary motion or pulsation at the period of the LSP. These two possibilities are now discussed.

#### 4.1. Binary Members?

Assuming the distribution of radial velocity shifts for non-LSPVs can be represented by the Gaussian distribution  $n \propto e^{-(v_r)^2/a^2}$ , then the curve for  $a = 1.3$  fits this distribution fairly well. This is the dotted curve shown in Figure 5. The solid curve in Figure 5 is the result of the following Monte Carlo simulation. The radial velocity distribution (RVD) for LSPVs is considered to be the result of two independent effects. The first is due to stellar pulsation and is represented by the RVD of the non-LSPVs. The second is due to orbital motion. A random radial velocity shift is drawn from the Gaussian RVD of the non-LSPVs. A second random radial velocity shift is calculated from a randomly selected inclination angle, orbital phase angle, reference orbital phase angle, and orbital separation (using eq. [19] in Han et al. 1995), given an average primary stellar mass and mass-ratio. The orbital phase angle is drawn from a distribution that depends on the orbital period, the length over which the stars were actually observed, in our case about 1 yr, and the

reference orbital phase angle. These two radial velocity shifts are then added. A set of such velocity shifts were calculated for binaries with an average primary mass of  $1.5 M_{\odot}$ , an average mass ratio of 0.33, separations greater than  $300 R_{\odot}$ , periods shorter than 18 yr (the maximum period in the sample is about 18 yr), and with the orbital plane within  $60^{\circ}$  of the line of sight. The resulting velocity shift distribution is the solid curve in Figure 5. This curve fits the RVD of the LSPVs well, showing that the larger radial velocity shifts of the LSPVs can be explained by assuming that these stars are in binary systems.

#### 4.2. Pulsation as the LSP?

To test whether pulsation is a possible explanation for the broader RVD of the LSPVs, a second Monte Carlo simulation was performed. Here it is again assumed that the RVD for LSPVs is the result of two independent effects, first pulsation at the primary pulsation period, and second pulsation at the LSP. The first effect was modeled as above. The second effect was modeled as a simple sinusoidal variation in stellar radius.

A random period was drawn from the observed LSP distribution. The LSP distribution can be fairly well

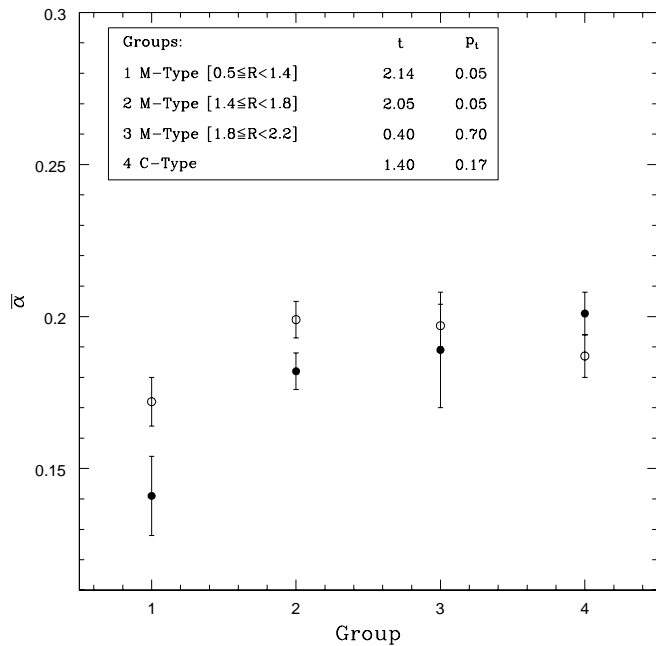


FIG. 4.—Mean value of the slope parameter  $\alpha$  for each group. Filled and open symbols refer to LSPVs and non-LSPVs, respectively. Error bars shows the standard error in the mean. Insert panel shows the definition of each group and the  $t$ -statistic with its associated significance,  $p_t$ , for each group. See text for details.

approximated by two uniform distributions, one with  $2.7 < \log(P) < 3.1$  and the other with  $3.1 < \log(P) < 3.6$ , with  $P$  in days, with 10 of the 28 stars having  $\log(P) > 3.1$  (ignoring V Hya in this case). Given a mean LSP pulsation amplitude (the difference between minimum and maximum radius), a random pulsation phase, and random reference pulsation phase, a velocity shift can be calculated. Again the

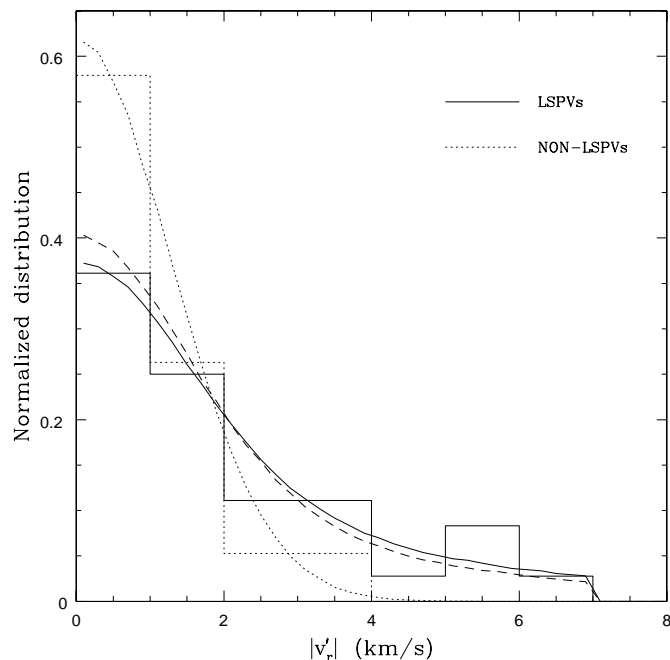


FIG. 5.—Normalized histogram of relative radial velocity (i.e., radial velocity change between two dates) for the two groups of stars. Curves are discussed in the text.

pulsation phase is drawn from a distribution that depends on the orbital period, the length over which the stars were actually observed, and the reference pulsation phase. This velocity shift was then combined with the velocity shift drawn from the RVD of the non-LSPVs. Assuming a mean LSP pulsation amplitude of  $100 R_{\odot}$  (roughly equivalent to assuming a velocity amplitude, minimum to maximum, of  $\sim 4.4 \text{ km s}^{-1}$ ), a whole set of such of such velocity shifts was generated. The resulting distribution of this set is shown by the dashed curve in Figure 5. This clearly shows that pulsation at an LSP is also a plausible explanation for the observed RVD of the LSPVs.

Hinkle et al. (2002) analyzed the radial velocity variations in nine northern LSPVs. They find that in six of these LSPVs the radial velocity seems to vary with periods similar to the photometric LSP. However, they find that assuming a binary hypothesis, five of these systems seem to have very similar “orbital” elements, with the remaining system having the largest uncertainty in its velocity curve. On the basis of this they reject the binary hypothesis and favor pulsation at a so far unknown mode, possibly of the type proposed by Wood (2000b) as a possible explanation for the observed photometric and radial velocity LSPs. Both the current study and that by Hinkle et al. (2002) clearly show that velocity variations, besides those due to normal mode pulsation, are associated with the LSP phenomenon in semi-regulars. The velocity variations associated with the LSP found by Hinkle et al. are in the same range as those shown for the LSPVs in Figure 5.

## 5. MID-INFRARED COLORS OF LSPVs

The suggestion by W99 that LSP minima are caused by obscuration by an orbiting dusty cloud or by periodic dust ejection leads to the possibility of differences in the mid-infrared colors between LSPVs and non-LSPVs: excess dust around the LSPVs would be expected to lead to excess mid-infrared emission. Figure 6 is an *IRAS* two-color diagram showing the LSPVs and non-LSPVs with reliable *IRAS* fluxes. The KS two-sample test gave no significant differences between mid-infrared colors for carbon-rich LSPVs and non-LSPVs. The same result is found for the oxygen-rich LSPVs and non-LSPVs. Also shown in Figure 6 is a sample of R Coronae Borealis (RCB) stars, taken from Clayton (1996), which have an *IRAS* counterpart. RCB stars are believed to undergo enhanced dust formation at irregular intervals, leading to the very deep minima observed in their light curves. This dust is believed to be amorphous carbon (see, e.g., Clayton 1996).

In Figure 6 some of the RCB stars lie in the same region as the LSPVs and non-LSPVs. These objects clearly do not have significant detectable excess mid-infrared emission as a result of their dust ejection episodes. However, some RCB stars do show excess mid-infrared emission. The absence of such emission from any of the LSPVs hints that dust may not be prominent in these systems. However, the similarity to some of the RCB stars makes this a rather weak statement. Hinkle et al. (2002) also point out the apparent absence of dust in the nine northern LSPVs they studied.

An alternative method for determining if the LSPVs have mid-infrared emission from circumstellar dust would be to compare the observed mid-infrared *IRAS* fluxes with the fluxes expected from a model atmosphere of the LSPV. However, in order to do this, an accurate  $T_{\text{eff}}$  and normaliz-

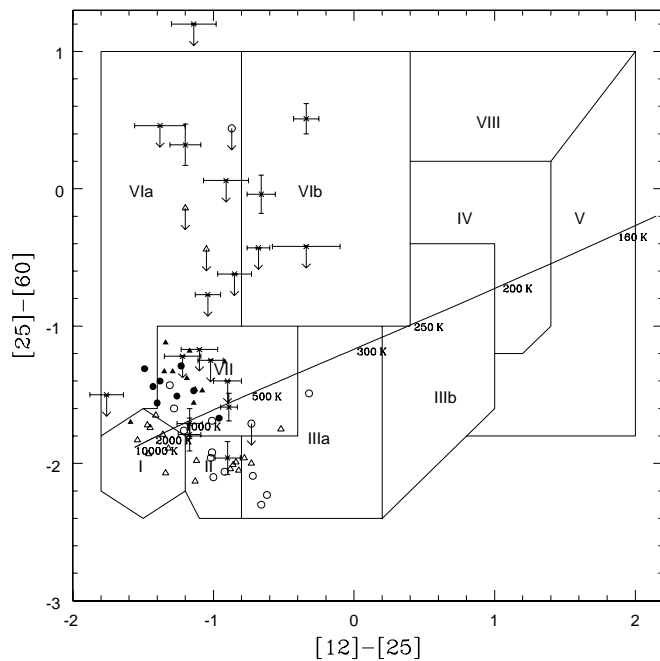


FIG. 6.—*IRAS* two-color diagram. Circles and triangles represent LSPVs and non-LSPVs, respectively. The filled and open symbols refer to carbon- and oxygen-rich objects, respectively. Crosses represent a sample of RCB stars (see text for details). Objects that have only an upper limit to the  $60\ \mu\text{m}$  flux are represented by a symbol with an arrow. Colors and regions in the diagram are those defined by Habing & van der Veen (1988). A blackbody line is shown, with temperatures indicated along it.

ing flux (e.g.,  $K$ ) at the time of the *IRAS* observations would be required. Since these quantities are not known for these variable stars, we were unable to use this method to check for excess mid-infrared flux.

## 6. SUMMARY AND CONCLUSIONS

High-resolution spectra of a sample of semiregular variables have been analyzed for velocity variation. It was found that the distribution of radial velocity variations for LSPVs is significantly broader than that for non-LSPVs and that this difference can be explained by assuming either that the LSPVs are in binary systems or are pulsating radially with an LSP. In the mean, the LSPVs do not seem to have broader spectral lines than non-LSPVs, suggesting that rotation is not the cause of the LSPs. In fact, a significant fraction of the LSPVs seem to have narrower lines than the non-LSPVs. Fourier analysis of the spectrum of V Hya confirms the result of Barnbaum et al. (1995) that this star has broadened lines but the results suggest that rotation alone is not a good model for explaining the line broadening. *IRAS* photometry shows no significant difference in mid-infrared colors between LSPVs, non-LSPVs, and many RCB stars that are known to be regularly ejecting dust. Hence, no definite conclusion can be drawn from *IRAS* data as to the presence of dust in LSPVs compared to non-LSPVs.

In summary, the results in this paper favor either binarity or pulsation as the cause of the LSPs in the  $\sim 25\%$  of semiregular variables in which they are observed. An ongoing monitoring program is being undertaken to obtain more spectra with good phase coverage. Hopefully, the resulting velocity curves, when compared to light curves and spectral type changes, will allow us to distinguish between these two possibilities.

This research has benefited from use of the SIMBAD database, operated at Centre de Données Astronomiques de Strasbourg, Strasbourg, France.

## REFERENCES

- Barnbaum, C., Morris, & M., Kahane, C. 1995, *ApJ*, 450, 862  
 Clayton, G. 1996, *PASP*, 108, 225  
 Gray, D. F. 1976, *The Observation and Analysis of Stellar Photospheres* (New York: Wiley)  
 Han, Z., Eggleton, P. P., Podsiadlowski, P., & Tout, C. A. 1995, *MNRAS*, 277, 1443  
 Hinkle, K. H., Lebzelter, T., Joyce, R. R., & Fekel, F. C. 2002, *AJ*, 123, 1002  
 Höfner, S., Feuchtinger, M. U., & Dorfi, E. A. 1995, *A&A*, 297, 815  
 Houk, N. 1963, *AJ*, 68, 253  
 Kholopov, P. N. 1985, *General Catalogue of Variable Stars* (4th ed.; Moscow: Nauka Publishing House) (GCVS)  
 Kiss, L. L., Szatmáry, K., Cadmus, R. R., Jr., & Mattei, J. A. 1999, *A&A*, 346, 542  
 Knapp, G. R., Dobrovolsky, S. I., Ivezić, Z., Young, K., Crosas, M., Mattei, J. A., & Rupen, M. P. 1999, *A&A*, 351, 97  
 Olivier, E., Whitelock, P., & Marang, F. 2001, *MNRAS*, 326, 490  
 Schwarzschild, M. 1975, *ApJ*, 195, 137  
 Soker, N., & Clayton, G. C. 1999, *MNRAS*, 307, 993  
 van der Veen, W. E. C. J., & Habing, H. J. 1988, *A&A*, 194, 125  
 Winters, J. M., Fleischer, A. J., Gauger, A., & Sedlmayr, E. 1994, *A&A*, 290, 623  
 Wood, P. R. 2000a, *Publ. Astron. Soc. Australia*, 17, 18  
 ———. 2000b, in *ASP Conf. Ser. 203, The Impact of Large Scale Surveys on Pulsating Star Research*, ed. L. Szabados & D. W. Kurtz (San Francisco: ASP), 379  
 Wood, P. R., et al. 1999, in *IAU Symp. 191, Asymptotic Giant Branch Stars*, ed. T. Le Bertre, A. Lébre, & C. Waelkens (San Francisco: ASP), 151 (W99)